REVIEW ARTICLE

Hypertrophic olivary degeneration in children: four new cases and a review of the literature with an emphasis on the MRI findings

[1]S E SANVERDI, MD, [1]K K OGUZ, MD and [2]G HALILOGLU, MD

[1]*Neuroradiology Division, Radiology Department School of Medicine, Hacettepe University, Ankara, Turkey, and* [2]*Pediatric Neurology, School of Medicine, Hacettepe University, Ankara, Turkey*

ABSTRACT. Injury to the dentato-rubro-olivary pathway causes hypertrophy and enlargement of the inferior olivary nuclei, which is called hypertrophic olivary degeneration (HOD). To date, adult cases of HOD have usually been reported, and there are only a few individual paediatric cases with limited radiological emphasis in the literature. We present the clinical and MRI findings of four new paediatric cases with HOD. Three of the patients had a posterior fossa surgery, and one did not have an identifiable cause.

Hypertrophic olivary degeneration (HOD) is a rare entity that develops after an injury to the dentato-rubro-olivary pathway (DROP) (also called the Guillain–Mollaret triangle, or GMT; Figure 1). Injury to the DROP causes hypertrophy and enlargement of the inferior olivary nuclei (ION), in contrast to the atrophy usually observed in other parts of the central nervous system (CNS) [1]. Oppenheim [2] first described the enlargement of the ION in his post-mortem study. Since then, a limited number of cases have been reported in the literature describing the histopathological, clinical and radiological features of this condition. Among these, paediatric cases constitute a minority in the literature. Thus, we intended to describe the clinical and radiological findings in four paediatric patients with HOD and to review the literature.

Case reports

Table 1 summarises the demographic data of our cases.

Case 1

This currently 6-year-old girl presented at the age of 3 years with a developmental delay, especially in expressing language. On MRI, there was increased signal intensity on the T_2 weighted images and a striking enlargement of the bilateral ION with a preserved shape and internal structure (Figure 2). No causative lesion in the GMT was observed. Hypertrophy and increased T_2 signal intensity of the ION persisted at the 1-year follow-up MRI. Her positron emission tomography (PET) scan revealed an increased metabolic activity in the brain stem and bilateral

basal ganglia. An electroencephalography study, serum and urine amino acids, and chromosomal analysis were normal. The patient has had special education and follow-up in another paediatric neurology clinic since then.

Case 2

A 17-year-old girl was admitted with a 3-month history of headache and imbalance as symptoms. Clinically, she had no neurological deficit. Her pre-operative cranial MRI showed a heterogeneous enhancing mass of $3 \times 3.5 \times 3$ cm in diameter located in the posterior surface of the fourth ventricle. The patient underwent surgery, during which the tumour was extracted subtotally. Pathological examination revealed World Health Organization (WHO) Grade IV medulloblastoma. On her first post-operative cranial MRI examination at 1 month, there was a small residual tumour on the left lateral wall of the fourth ventricle. In the same study, T_2 signal increase on both of the dentate nuclei and T_2 signal loss suggestive of late subacute or chronic haemorrhage on the right dentate nucleus were observed. Slight enlargement and prominent T_2 hyperintensity on both ION were present as well (Figure 3). Follow-up MRI at the sixth month revealed a marked bilateral olivary hypertrophy on the right. Bilateral HOD was associated with a chronic haemorrhage and volume loss of the dentate nuclei. One-year follow-up MR study revealed the disappearance of the residual tumour after radio- and chemotherapy, and of the sequela of the surgery in the posterior fossa.

Case 3

A 3-year-old boy was admitted to an outside hospital with the symptoms of gait ataxia and imbalance, and had been diagnosed with posterior fossa tumour. He had

Address correspondence to: Dr Eser Sanverdi, Radiology Department, School of Medicine, Hacettepe University, 06100 Sihhiye, Ankara, Turkey. E-mail: esersanverdi@yahoo.com
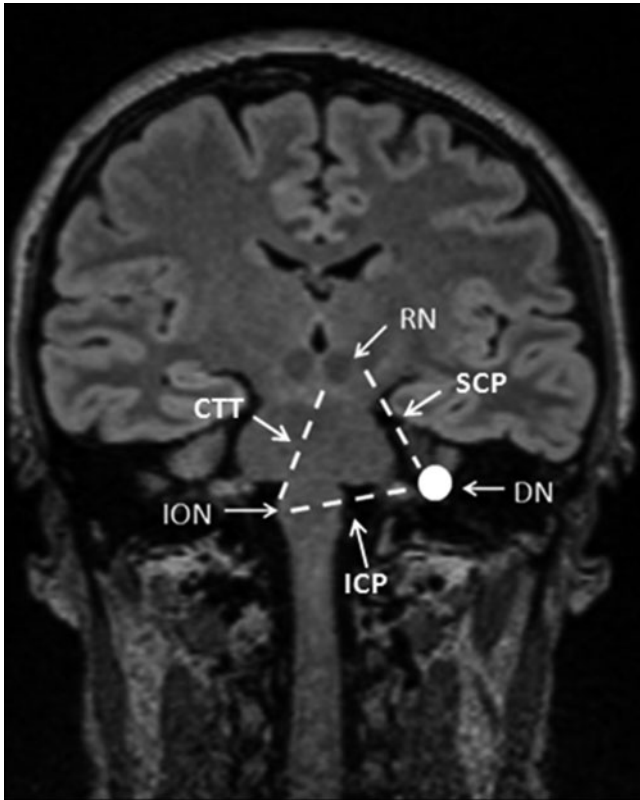
Figure 1. Illustration of the Guillain–Mollaret triangle by a coronal T_1 weighted MR image. CTT, central tegmental tract; DN, dentate nucleus; ICP, inferior cerebellar peduncle; ION, inferior olivary nucleus; RN, red nucleus; SCP, superior cerebellar peduncle.

been operated on, and pathological examination of the tumour had revealed WHO Grade IV medulloblastoma. Later, he received radio- and chemotherapy at our institution. In his pre-operative cranial MRI, a heterogeneous tumour in the fourth ventricle of $4 \times 4.5 \times 3.5$ cm in size was seen. In his first post-operative cranial MR study at 2 months following the surgery, atrophy and increased T_2 signal of the left superior cerebellar peduncle and enlarged and remarkable T_2 hyperintense bilateral olives were observed, in addition to the post-surgical changes in the posterior fossa. Olivary hypertrophy also appeared bilaterally in the second-year follow-up MRI. Hypertrophy was found to be present in his long-term (6-year) follow-up (Figure 4). Neither residual nor recurrent tumour was seen. Neurological examination at the age of 10 years was normal except for a right-sided esotropia.

Case 4

This 6-year-old boy had been operated on in an outside hospital for a posterior fossa tumour and was diagnosed with medulloblastoma. After the surgery, he applied to our institution for adjuvant therapy and follow-up. Pre-operative images could not be obtained. In his post-operative MR examination performed 2 months following the surgery, no mass was observed, but bilateral HOD was more prominent on the left owing to the injury of the right superior cerebellar peduncle. In the following 3 consecutive years, olivary hypertrophy resolved progressively, and at the end of the fourth year, the olives were atrophic, as assessed by MRI.

Discussion

The anatomical triangle named after Guillain and Mollaret consists of the ipsilateral red nucleus, the inferior olivary nucleus (which has connections through the central tegmental tract) and the contralateral dentate nucleus. The superior cerebellar peduncle provides connection between the ipsilateral red and the contralateral dentate nuclei, while the inferior cerebellar peduncle links the contralateral dentate and the ipsilateral and inferior olivary nuclei and makes the other edges of the triangle (Figure 1) [3–5]. Lesions deafferating the olive (in the dentato-rubral or rubro-olivary pathway) can result in HOD more frequently than lesions of the olivo-dentate pathway [6].

HOD is almost always unilateral; however, rare bilateral cases have been reported. Midline lesions or lesions in the brachium conjunctivum (superior cerebellar peduncle), finally interrupting decussation of the DROP, can result in bilateral HOD [3, 5]. Our small paediatric series is distinguished from the previous studies in that all cases presented with bilateral HOD. In Case 1, the patient with bilateral HOD had no visible lesion in DROP in just two MR studies performed with an interval of 1 year. Despite the fact that she had no clinical manifestation of HOD, she was accepted with a diagnosis of ''idiopathic degeneration of the ION'' according to the MR findings. Although a few reports in the literature state that metronidazole-induced encephalopathy could be represented as HOD in adulthood [7–9], there is no case of idiopathic HOD in the English-language literature to the best of our knowledge. Damage to the bilateral dentate nuclei in Case 2, and to the unilateral superior cerebellar peduncles in Cases 3 and 4, was suspected to be the cause of the bilateral

Table 1. Demographic data of our cases

Case number	Age of patient/gender	Aetiology	Site of causative lesion	Lateralisation of HOD	Time to first MRI displaying HOD
1	3/F	Idiopathic	–	B	In second month of clinical presentation
2	17/F	Posterior fossa tumour resection	Bilateral dentate nucleus	B	1 month after the surgery
3	3/M	Posterior fossa tumour resection	Left superior cerebellar peduncle	B	2 months after the surgery
4	3/M	Posterior fossa tumour resection	Right superior cerebellar peduncle	B	2 months after the surgery

B, bilateral; F, female; HOD, hypertrophic olivary degeneration; M, male.
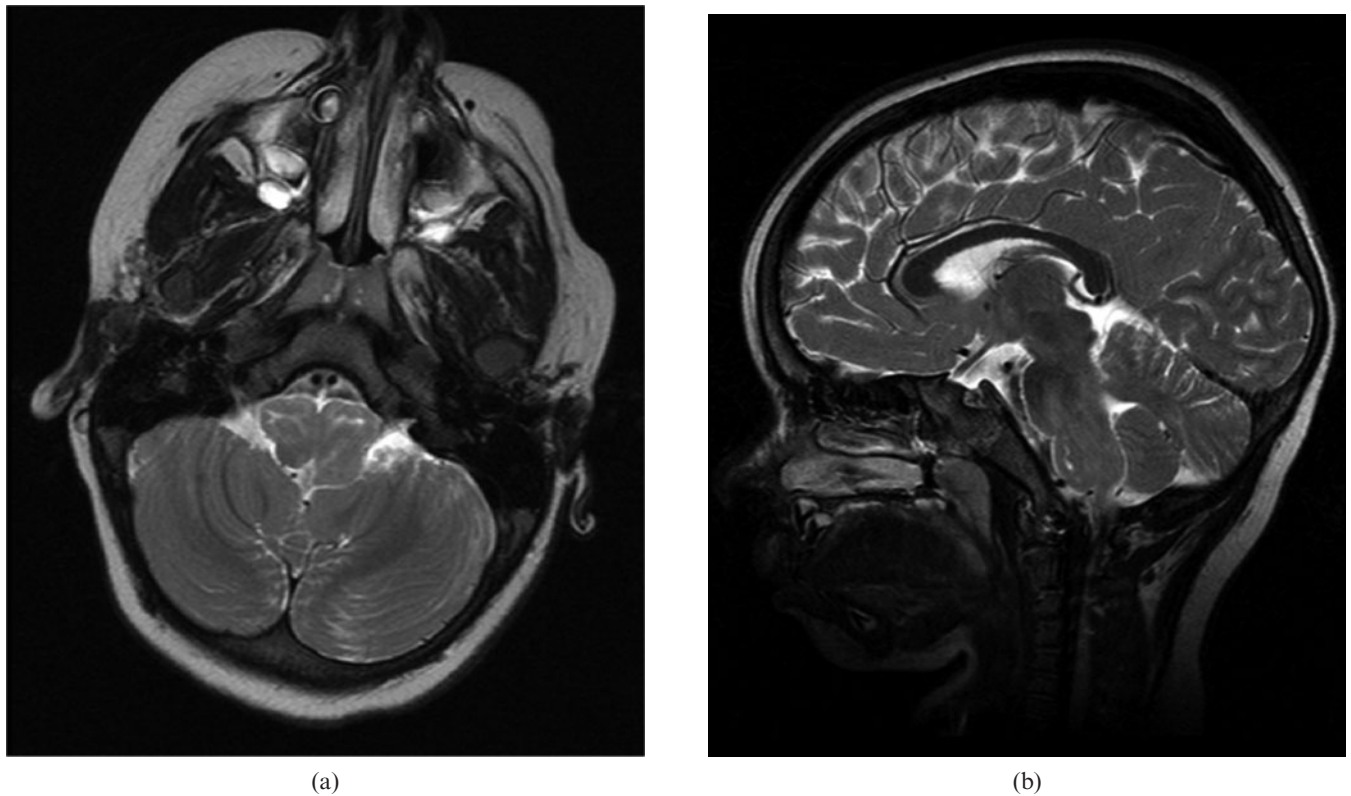
Figure 2. Case 1. Bilateral inferior olivary nuclei hypertrophy and increased signal intensity are seen on the (a) axial and (b) sagittal T_2 weighted (repetition time/echo time, 3800/90 ms) images. Note the preserved shape of the nuclei on axial images.
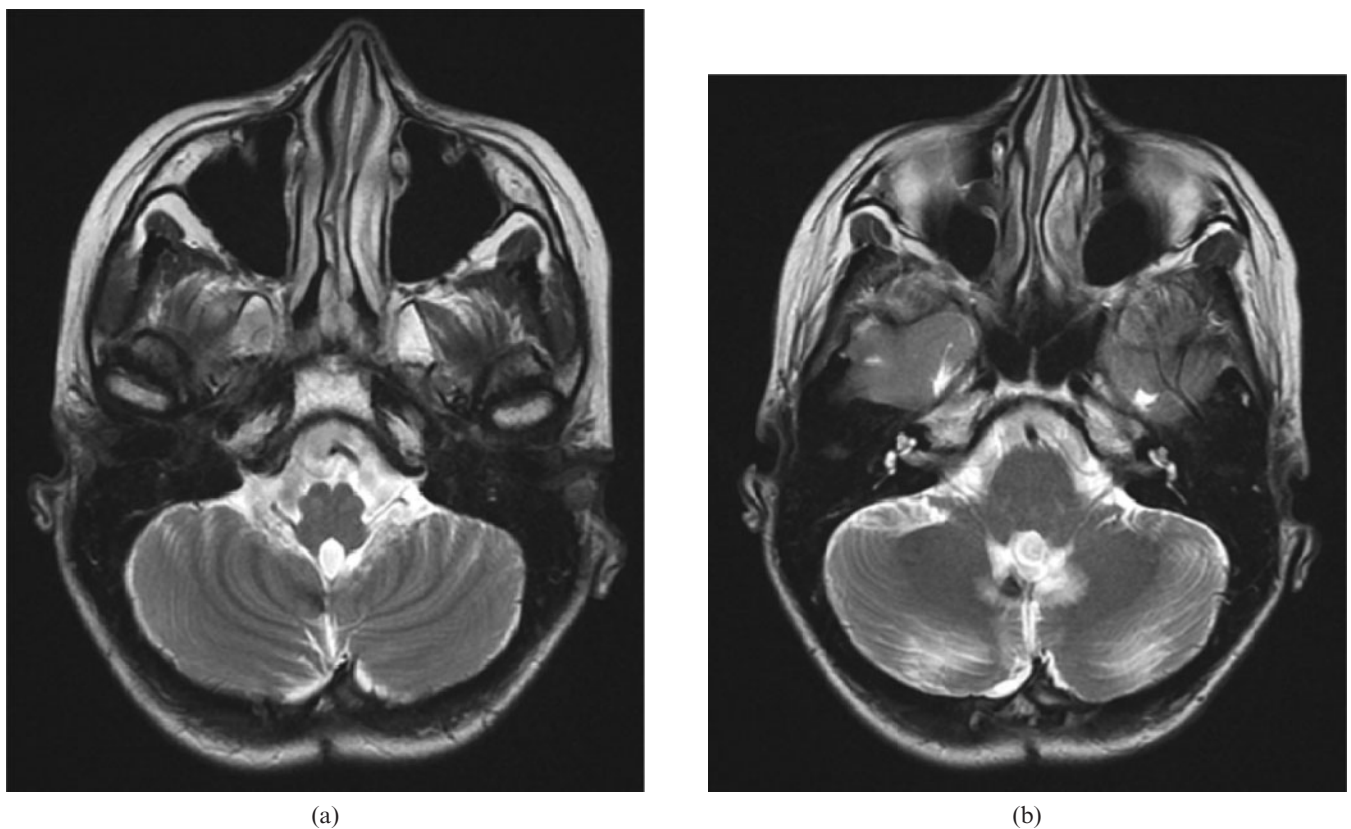

Figure 3. Case 2. (a) Increased signal intensity and enlargement of the inferior livery nuclei are seen in the first post-operative axial T_2 weighted (repetition time/echo time (TR/TE), 3800/90 ms) MR image as being the causative lesions. (b) The gliotic changes in both dentate nuclei and additional haemorrhagic signal loss in the right dentate nucleus are seen on the same axial T_2 weighted (TR/TE, 3800/90 ms) MR image.
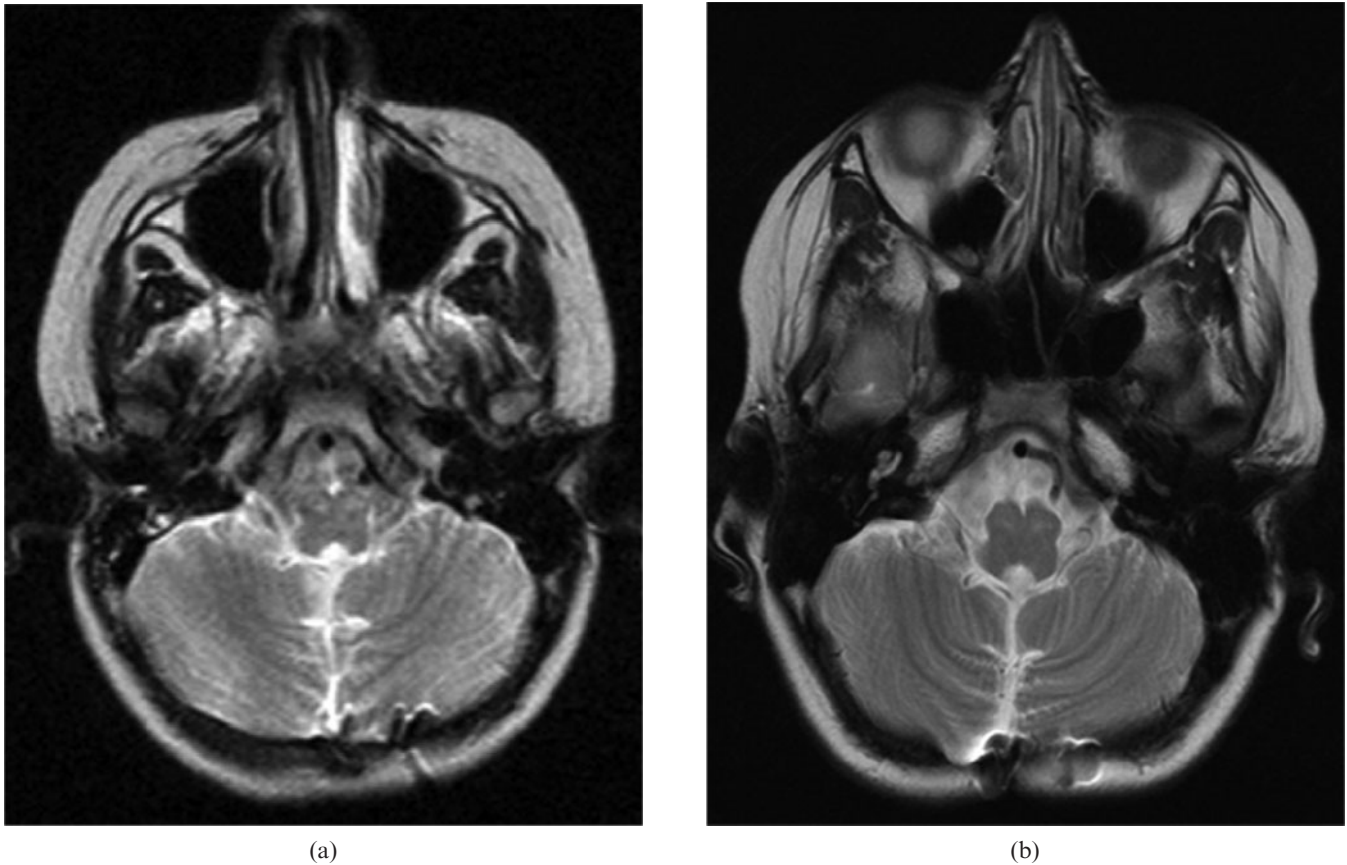
(a)   (b)

Figure 4. Case 3. (a) Increased signal intensity and enlargement of the inferior olivary nuclei are seen in first post-operative axial T_2 weighted (repetition time/echo time, 3800/90 ms) MR image obtained at 3 months following the surgery. (b) At the sixth-year follow-up imaging, hypertrophy and T_2 hyperintensity persist.

HOD. In all cases except the idiopathic one, surgery-related injuries were present. This aetiological frequency differs in the adult population, in which ischaemic lesions (most often along with haemorrhage) are the leading cause [5].

Although neuronal loss and glial proliferation typically follow tissue damage in the CNS, degeneration of the ION occurs with hypertrophy [3, 5, 10]. Pathological studies of HOD have demonstrated vacuolar degeneration, neuronal enlargement, astrocyte hypertrophy and gliosis [3]. Ultrastructural electron microscopic studies have shown that increased neuronal size could be attributed to neurofilamentous proliferation and cytoplasmic vacuolisation to the formation of rough endocytoplasmic reticulum vesicles [11]. A striking proliferation of mitochondria in the glial cells can be related to the increased metabolic activity shown by PET in the early stages of HOD [12]. Similarly, single photon emission CT revealed hyperperfusion of the right ION, left thalamus and dentate nuclei in a patient who developed a palatal tremor (PT) 2 months after brain stem tumour surgery as reported by Kim et al [13]. Our first patient had increased metabolic activity in the ION and bilateral basal ganglia on PET. With no symptoms attributable to HOD, such as prominent hypertrophy of the ION, we believe that our patient (Case 1) was in the early stage [12]. Although a 1-year follow-up MR study revealed no structural interval change, we could not obtain a follow-up PET scan to observe the evolution of the metabolic changes.

Previous reports on hypertrophic olivary degeneration

Features of the previous reports on HOD are given in Table 2. In a report published in 1998, a 14-year-old girl who had been operated on because of a left pontine tegmentum cavernous angioma developed left HOD, as documented by MRI 13 months after the surgery. However, neither her clinical symptoms nor the follow-up reports of the patients were given in the report [5]. In Birbamer et al's [14] report by age range (5–69 years), we realised that some paediatric cases had been involved, but there were no additional data. Among seven patients in a series by Bontozoglou et al [4], two were of paediatric age (*i.e.* 8 and 9 years old). These two cases with PT had medulloblastoma involving the unilateral dentate nucleus on pre-operative and contralateral red nucleus atrophy on post-operative imaging [4]. Among our patients, the dentate nuclei and the superior cerebellar peduncles were affected. We did not find visible atrophy or signal abnormality of the red nuclei in our cases.

A common feature between the two paediatric HOD cases following head trauma, reported by Suzuki et al [15] and our series, is the lack of PT clinically. This suggests that because this characteristic clinical finding may not be present, recognition of the condition on MRI becomes even more important in order to avoid an erroneous diagnosis of tumour or other space-occupying lesions of the medulla oblongata.

Table 2. Summary of comparison of other studies

Author (year)	Number of cases	Age/gender of patients	Aetiology	Site of causative lesion	Lateralisation of HOD	Time to first MRI displaying HOD
Dinçer et al (2011) [1]	1	16/F	CTT cavernoma	CTT ($n=1$)	L ($n=1$)	NA
Bontozoglou et al (1991) [4]	2	8, 9/NA, NA	DN tumour excision	R DN ($n=2$)	L ($n=2$)	1 month after the surgery
Phatouros and McConachie (1998) [5]	1	14/F	L pontin tegmentum cavernoma	CTT ($n=1$)	L ($n=1$)	13 months after the surgery
Birbamer et al (1994) [14]	NA	NA/NA	NA	NA	NA	NA
Suzuki et al (1999) [15]	2	12, 17/M, F	Trauma	CTT ($n=2$)	R ($n=1$), L ($n=1$)	2–4 months after the insult
Present study	4	3, 17, 3, 3/F, F, M, M	Idiopathic ($n=1$), posterior fossa tumour resection ($n=3$)	SCP ($n=2$), DN ($n=1$), no lesion ($n=1$)	B ($n=4$)	1–2 months after the surgery (except Case 1)

B, bilateral; CTT, central tegmental tract; DN, dentate nucleus; HOD, hypertrophic olivary degeneration; L, left; NA, not available; OPT, oculopalatal tremor; R, right; SCP, superior cerebellar peduncle.

Whether the pathological time course of HOD can be considered in six stages, as described by Hornyak et al [10] and Goto and Kaneko [16], or in three stages, as described by Ash and Srinivasan [3], both histological and radiological changes begin to appear approximately 3 weeks after the injury. Jellinger [17] reported that early vacuolation occurring with in 15–20 days was responsible for the T_2 signal increase also seen around the third week following tissue damage. Olivary enlargement follows T_2 hyperintensity and can persist for years. However, the whole degenerative process is usually known to take more than a year, and finally atrophy of the ION develops [16, 18]. One may expect that once atrophy and gliosis occur in the final stage, T_2 hyperintensity may persist indefinitely [3, 5, 10, 18]. Regular temporal changes in the size and signal intensity of the ION consistent with the literature were observed in all the patients presented in this report. As an exception, Case 3 presented MRI findings of HOD for 6 years, which is longer than any report in the paediatric literature.

None of our patients had PT and/or ocular oscillopsia as clinical manifestations of HOD. Based on their clinicopathological correlative study, Nishie et al [19] stated that symptomatic PT was not correlated with inferior olivary hypertrophy, but instead with the loss of GABAergic inhibitory fibres in the dentato-olivary pathway [20, 21]. A similar imbalance of neurotransmitters may be present in the pathophysiology of asymptomatic paediatric patients, as in our series. When PT is associated with pendular nystagmus, it is called OPT. OPT is a delayed complication of the damage to part of the DROP/GMT except for the dorsal cap of the ION, the dorsolateral reticular formation or the paramedian tract cell groups [22–24].

Our patients with HOD can be distinguished from previous studies in some aspects. Despite its limited size, this study constitutes the largest series with the youngest patients in the English-language literature. Additionally, we realise that characteristic clinical features of HOD such as PT and ocular oscillopsia may not be present in children. Given that most of the paediatric cases had posterior fossa surgery for the tumours, recognition of the imaging findings of HOD is important to avoid interpretation of this entity as a recurrent tumour, a new ischaemic event or other space-occupying lesions.

Conclusion

HOD is a rare transsynaptic degeneration that usually appears at around 3 weeks following an injury to the Guillian–Mollaret triangle. T_2 hyperintensity and enlargement of the ION are the radiological hallmarks of this entity. On follow-up imaging, the ION can be atrophic or hypertrophic and can persist for years. Patients may represent no clinical manifestations attributable to HOD. Thus, it is important to recognise radiological findings, especially in such young patients, in order to avoid misinterpretation of this benign condition.

References

1. Dinçer A, Özyurt O, Kaya D, Koşak E, Öztürk C, Erzen C, et al. Diffusion tensor imaging of Guillain-Mollaret triangle in patients with hypertrophic olivary degeneration. J Neuroimaging 2011;21:145–51.
2. Oppenheim H. Uber Olivendegeneration bei Atheromatese der basalen Hirnarterien. Berl Klin Wschr 1887;34:638–9,
3. Ash L, Srinivasan A. Case of the season: hypertrophic olivary degeneration. Semin Roentgenol 2008;43:171–2.
4. Bontozoglou NP, Chakeres DW, Martin GF, Brogan MA, McGhee RB. Cerebellorubral degeneration after resection of cerebellar dentate nucleus neoplasms: evaluation with MR imaging. Radiology 1991;180:223–8.
5. Phatouros CC, McConachie NS. Hypertrophic olivary degeneration: case report in a child. Pediatr Radiol 1998;28:830–1.
6. Harter DH, Davis A. Hypertrophic olivary degeneration after resection of a pontine cavernoma. Case illustration. J Neurosurg 2004;100:717.
7. Seok JI, Yi H, Song YM, Lee WY. Metronidazole-induced encephalopathy and inferior olivary hypertrophy: lesion analysis with diffusion-weighted imaging and apparent diffusion coefficient maps. Arch Neurol 2003;60:1796–800.
8. Kim E, Na DG, Kim EY, Kim JH, Son KR, Chang KH. MR imaging of metronidazole-induced encephalopathy: lesion

distribution and diffusion-weighted imaging findings. AJNR Am J Neuroradiol 2007;28:1652–8.

9. Cazals X, Omoumi P, Agnard P, Bibi R, Ferquel C, Cazeneuve N, et al. [Reversible metronidazole-induced encephalopathy and hypertrophic olivary degeneration]. J Radiol 2010;91:304–6.

10. Hornyak M, Osborn AG, Couldwell WT. Hypertrophic olivary degeneration after surgical removal of cavernous malformations of the brain stem: report of four cases and review of the literature. Acta Neurochir (Wien) 2008;150: 149–56.

11. Kurachi M, Nakamura I, Katsukawa K, Kobayashi K, Sano Y, Isaki K, et al. Olivary hypertrophy in a case with palatal myoclonus: light- and electron-microscopic study. Folia Psychiatr Neurol Jpn 1985;39:543–50.

12. Dubinsky RM, Hallett M, Di Chiro G, Fulham M, Schwankhaus J. Increased glucose metabolism in the medulla of patients with palatal myoclonus. Neurology 1991;41:557–62.

13. Kim SJ, Lee WY, Kim BJ, Kim JY, Hong SB, Tae WS, et al. Isolated tongue tremor after removal of cerebellar pilocytic astrocytoma: functional analysis with SPECT study. Mov Disord 2007;22:1825–8.

14. Birbamer G, Gerstenbrand F, Aichner F, Buchberger W, Chemelli A, Langmayr J, et al. MR-imaging of post-traumatic olivary hypertrophy. Funct Neurol 1994;9: 183–7.

15. Suzuki M, Takashima T, Ueda F, Fujinaga Y, Horichi Y, Yamashita J. Olivary degeneration after intracranial haemorrhage or trauma: follow-up MRI. Neuroradiology 1999;41:9–12.

16. Goto N, Kaneko M. Olivary enlargement: chronological and morphometric analyses. Acta Neuropathol 1981;54:275–82.

17. Jellinger K. Hypertrophy of the inferior olives. Report on 29 cases. Z Neurol 1973;205:153–74.

18. Kitajima M, Korogi Y, Shimomura O, Sakamoto Y, Hirai T, Miyayama H, et al. Hypertrophic olivary degeneration: MR imaging and pathologic findings. Radiology 1994;192:539–43.

19. Nishie M, Yoshida Y, Hirata Y, Matsunaga M. Generation of symptomatic palatal tremor is not correlated with inferior olivary hypertrophy. Brain 2002;125:1348–57.

20. Sotelo C, Gotow T, Wassef M. Localization of glutamic-acid-decarboxylase-immunoreactive axon terminals in the inferior olive of the rat, with special emphasis on anatomical relations between GABAergic synapses and dendrodendritic gap junctions. J Comp Neurol 1986;252:32–50.

21. De Zeeuw CI, Simpson JI, Hoogenraad CC, Galjart N, Koekkoek SK, Ruigrok TJ. Microcircuitry and function of the inferior olive. Trends Neurosci 1998;21:391–400.

22. Matsuo F, Ajax ET. Palatal myoclonus and denervation supersensitivity in the central nervous system. Ann Neurol 1979;5:72–8.

23. Guillain G. The syndrome of synchronous and rhythmic palato-pharyngo-laryngo-oculo-diaphragmatic myoclonus: (section of neurology). Proc R Soc Med 1938;31:1031–8.

24. Kim JS, Moon SY, Choi KD, Kim JH, Sharpe JA. Patterns of ocular oscillation in oculopalatal tremor: imaging correlations. Neurology 2007;68:1128–35.